

## DISCOVERY OF THE TRANSIENT MAGNETAR 3XMM J185246.6+003317 NEAR SUPERNOVA REMNANT KESTEVEN 79 WITH XMM-Newton

PING ZHOU<sup>1,2</sup>, YANG CHEN<sup>1,3</sup>, XIANG-DONG LI<sup>1,3</sup>, SAMAR SAFI-HARB<sup>2,4</sup>, MARIANO MENDEZ<sup>5</sup>, YUKIKATSU TERADA<sup>6</sup>,  
WEI SUN<sup>1</sup>, AND MING-YU GE<sup>7</sup>

Accepted to *ApJL* on 2013 December 10

### ABSTRACT

We report the serendipitous discovery with XMM-Newton that 3XMM J185246.6+003317 is an 11.56 s X-ray pulsar located 1' away from the southern boundary of supernova remnant Kes 79. The spin-down rate of 3XMM J185246.6+003317 is  $< 1.1 \times 10^{-13} \text{ ss}^{-1}$ , which, together with the long period  $P = 11.5587126(4) \text{ s}$ , indicates a dipolar surface magnetic field of  $< 3.6 \times 10^{13} \text{ G}$ , a characteristic age of  $> 1.7 \text{ Myr}$ , and a spin-down luminosity of  $< 2.8 \times 10^{30} \text{ erg s}^{-1}$ . Its X-ray spectrum is best-fitted with a resonant Compton scattering model and can be also adequately described by a blackbody model. The observations covering a seven month span from 2008 to 2009 show variations in the spectral properties of the source, with the luminosity decreasing from  $2.8 \times 10^{34} \text{ erg s}^{-1}$  to  $4.7 \times 10^{33} \text{ erg s}^{-1}$ , along with a decrease of the blackbody temperature from  $kT \approx 0.8 \text{ keV}$  to  $\approx 0.6 \text{ keV}$ . The X-ray luminosity of the source is higher than its spin-down luminosity, ruling out rotation as a power source. The combined timing and spectral properties, the non-detection of any optical or infrared counterpart, together with the lack of detection of the source in archival X-ray data prior to the 2008 XMM-Newton observation, point to 3XMM J185246.6+003317 being a newly discovered transient low-B magnetar undergoing an outburst decay during the XMM-Newton observations. The non-detection by Chandra in 2001 sets an upper limit of  $4 \times 10^{32} \text{ erg s}^{-1}$  to the quiescent luminosity of 3XMM J185246.6+003317. Its period is the longest among currently known transient magnetars. The foreground absorption toward 3XMM J185246.6+003317 is similar to that of Kes 79, suggesting a similar distance of  $\sim 7.1 \text{ kpc}$ .

*Subject headings:* pulsars: individual (3XMM J185246.6+003317)– stars: magnetars

### 1. INTRODUCTION

Anomalous X-ray pulsars (AXPs) and soft gamma-ray repeaters (SGRs) have been recognized as manifestations of a small class of known neutron stars dubbed “magnetars”, commonly believed to be powered by the decay of their strong magnetic fields (Thompson & Duncan 1995, 1996; Thompson et al. 2002). Nearly two decades of observations show that this population of objects rotate slowly in comparison to the classical rotation-powered pulsars, with periods  $P \sim 2\text{--}12 \text{ s}$ , large period derivatives  $\dot{P} \sim 10^{-13}\text{--}10^{-10} \text{ ss}^{-1}$ , and highly variable X-ray emission. Their X-ray luminosities are notably larger than their rotational energy loss, implying that their powering mechanism cannot be rotation but rather magnetic field decay, with surface dipole magnetic fields (inferred from  $P$  and  $\dot{P}$ ) exceeding the quantum critical value  $B_{\text{QED}} = 4.4 \times 10^{13} \text{ G}$  (for reviews, see Mereghetti 2008, 2013; Rea & Esposito 2011; Rea 2013). Other models

have been also proposed to explain magnetars, including accretion from a fallback disk (Alpar et al. 2013) or quark stars (Ouyed et al. 2007). To date, there are only 26 known magnetars<sup>8</sup> (Olausen & Kaspi 2013). Despite being a small sample among the known neutron star population, magnetars have attracted wide and growing interest in the last decade, among both the observational and theoretical communities, continually providing us with surprises and unexpected discoveries that are shaping our understanding of the diversity of neutron stars and blurring the distinction between them.

This growing diversity includes, in addition to the magnetars and “classical” rotation-powered pulsars, high-B radio pulsars, rotating radio transients, X-ray dim isolated neutron stars, and the central compact objects (CCOs), with the latter recently dubbed as “anti-magnetars” and showing evidence for a much lower magnetic field ( $\sim 10^{10}\text{--}10^{11} \text{ G}$ ; Gotthelf et al. 2013). A number of recent observations showed that a super-critical dipole magnetic field ( $B \geq B_{\text{QED}}$ ) is not necessary for neutron stars to display magnetar-like behavior (e.g., the discoveries of two low-B magnetars: SGR 0418+5729 and Swift J1822.3–1606; Rea et al. 2010, 2012; Scholz et al. 2012), that magnetars can be also radio emitters (e.g., Camilo et al. 2006), and that one high-B pulsar (PSR J1846–0258 in supernova remnant (SNR) Kes 75), thought to be an exclusively rotation-powered radio pulsar, behaved like a magnetar (Kumar & Safi-Harb 2008; Gavriil et al. 2008). Moreover, the discovery of

<sup>1</sup> Department of Astronomy, Nanjing University, Nanjing 210093, China

<sup>2</sup> Department of Physics and Astronomy, University of Manitoba, Winnipeg, MB R3T 2N2, Canada

<sup>3</sup> Key Laboratory of Modern Astronomy and Astrophysics, Nanjing University, Ministry of Education, China

<sup>4</sup> Canada Research Chair

<sup>5</sup> Kapteyn Astronomical Institute, University of Groningen, P.O. Box 800, 9700 AV Groningen, the Netherlands

<sup>6</sup> Graduate School of Science and Engineering, Saitama University, 255 Simo-Ohkubo, Sakura-ku, Saitama 338-8570, Japan

<sup>7</sup> Key Laboratory for Particle Astrophysics, Institute of High Energy Physics, Chinese Academy of Sciences, Beijing 100049, China

<sup>8</sup> <http://www.physics.mcgill.ca/~pulsar/magnetar/main.html>

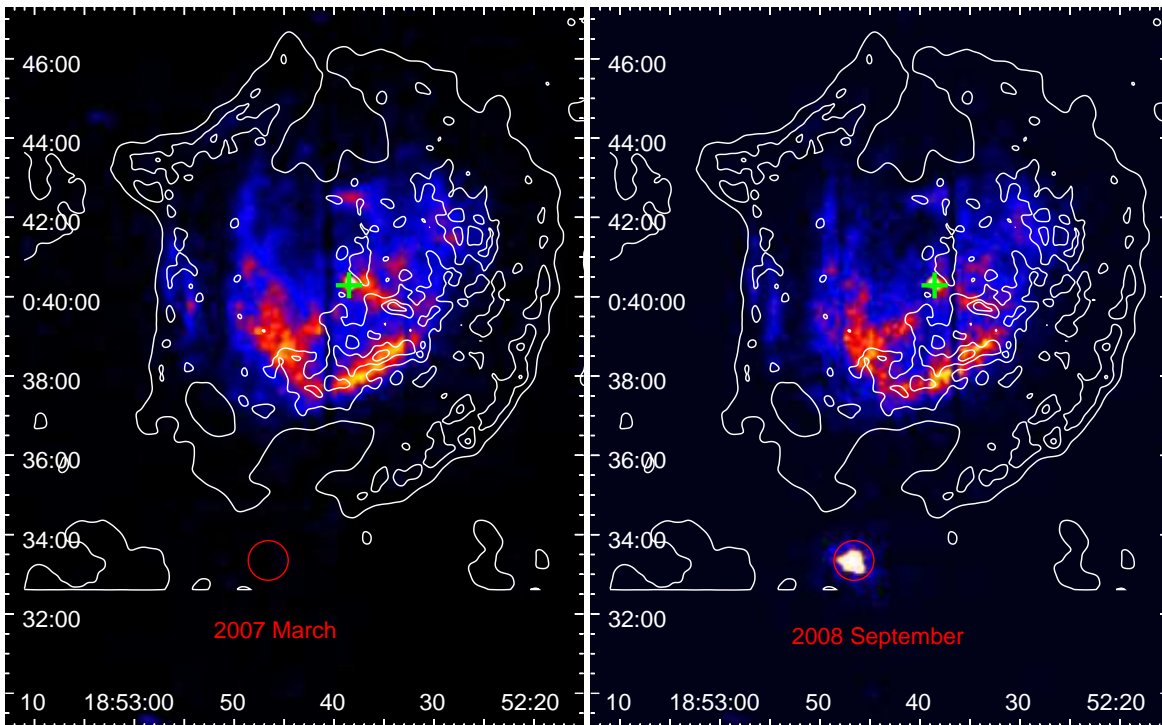


FIG. 1.— Raw EPIC-MOS2 image of 3XMM J185246.6+003317 and the northern SNR Kes 79 from the observations taken during 2007 March 20–21 (Obs ID 0400390301, left panel) and 2008 September 23 (Obs ID 0550670401, right panel), respectively. The images have been smoothed using a Gaussian with  $\sigma=3$  and are shown with the same intensity scale. Radio contours are overlaid using Very Large Array 1.4 GHz continuum emission. The red circle and the green cross indicate the locations of the transient magnetar and the CCO, respectively.

a handful of transient magnetars (i.e., previously missing magnetars discovered following an outburst typified by XTE J1810–197; Ibrahim et al. 2004) are showing us that there is likely a large population of magnetars awaiting discovery.

Among the current known magnetars, eight have been so far identified as transient magnetars (XTE J1810–197, AX J1845–0258, CXOU J164710.2–455216, 1E 1547–5408, SGR 1627–41, SGR 1745–29, SGR 0501+4516, and PSR J1622–4950), the study of which is providing a wealth of information about the emission mechanisms and evolution of these objects, as well as their connection to the other classes of neutron stars (Rea & Esposito 2011). Any new addition would be important to increase this small sample and provide physical insights on their physical properties.

In this Letter, we report on the *XMM-Newton* discovery of a transient low-B magnetar located south of SNR Kes 79 hosting a CCO (Seward et al. 2003). This source was serendipitously discovered during our multi-wavelength study of Kes 79 (P. Zhou et al. in preparation; Chen et al. 2013), adding a new member to the growing class of transient magnetars.

## 2. OBSERVATIONS

The observations described here were carried out with *XMM-Newton* pointing at SNR Kes 79 using the European Photon Imaging Camera (EPIC) which is equipped with one pn (Strüder et al. 2001) and two MOS cameras (Turner et al. 2001) covering the 0.2–12 keV energy range.

We found a bright point-like source just outside the southern boundary of the remnant in the 2008–2009 observations (see below) at around the following coordinates (J2000): R.A. =  $18^{\text{h}}52^{\text{m}}46^{\text{s}}.6$  decl. =  $00^{\circ}33'20''.9$ , located  $7''.4$  away from the CCO (see Figure 1). Checking against the *XMM-Newton* Serendipitous Source Catalogue,<sup>9</sup> we find a point source (3XMM J185246.6+003317) which coincides with the above-mentioned source. Therefore, we will refer to the source hereafter by its 3XMM name.

The field around this source was covered on several occasions spanning 2004–2007 and in 2008 and 2009. We selected 12 archival *XMM-Newton* observations carried out during 2008–2009 (PI J. Halpern) for our detailed analysis (see the observation information in Table 1). Here we only use the data collected with EPIC-MOS2, which happened to cover 3XMM J185246.6+003317 during both the 2008 and 2009 observations. All the MOS observations were carried out in the full frame mode with a time resolution of 2.6 s. After removing the time intervals and observations with heavy proton flares, the total effective exposure time for the MOS2 observations amounts to 273 ks. We used the flare-unscreened data to analyze the periodicities and the spin-down rate, while the flare-screened data are used for other analyses. The observation taken on 2009 March 25 (ObsID 0550671101) suffered from contamination by proton flares during most of the observation time and hence was only used for determining the periodicity and the spin-down rate. While

<sup>9</sup> <http://xmmssc-www.star.le.ac.uk/Catalogue/3XMM-DR4/UserGuide-xmmcat.html>

TABLE 1  
SUMMARY OF THE 12 *XMM-Newton* EPOCH OBSERVATIONS, THEIR TIMING AND SPECTRAL PROPERTIES

ObsID	Obs. Date	Exposure <sup>a</sup> (ks)	Start Epoch <sup>b</sup> (MJD)	Period <sup>c</sup> (s)	$f_p$ %	<i>power-law</i>		<i>bbodyrad</i>		<i>RCS</i>	
						$\Gamma$	$kT_{\text{bb}}$ (keV)	$R_{\text{bb}}$ (km)	$kT_{\text{RCS}}$ (keV)	$F_X$ ( $10^{-12}$ erg cm $^{-2}$ s)	
0550670201	2008 Sep 19	21.6/21.6	54728.75	11.55856 (14)	62 ± 7	3.30 ± 0.08	0.78 ± 0.02	0.70 ± 0.04	0.69 $^{+0.02}_{-0.06}$	3.9 ± 0.8	
0550670301	2008 Sep 21	30.3/30.3	54730.07	11.55853 (7)	64 ± 6	3.14 ± 0.08	0.80 ± 0.02	0.71 ± 0.03	0.72 $^{+0.02}_{-0.05}$	4.4 ± 0.8	
0550670401	2008 Sep 23	35.4/35.4	54732.07	11.55879 (7)	62 ± 5	3.18 ± 0.08	0.79 ± 0.02	0.74 ± 0.03	0.71 $^{+0.02}_{-0.06}$	4.6 ± 0.9	
0550670501	2008 Sep 29	33.3/33.3	54738.01	11.55865 (7)	56 ± 6	3.14 ± 0.08	0.81 ± 0.02	0.74 ± 0.03	0.72 $^{+0.02}_{-0.05}$	5.0 ± 0.9	
0550670601	2008 Oct 10	35.6/30.5	54750.01	11.55870 (7)	68 ± 6	3.30 ± 0.08	0.78 ± 0.02	0.70 ± 0.04	0.69 $^{+0.02}_{-0.06}$	3.9 ± 0.8	
0550670901	2009 Mar 17	26.2/23.3	54907.60	11.55854 (35)	58 ± 11	3.85 ± 0.24	0.63 ± 0.04	0.51 ± 0.07	0.54 ± 0.03	0.8 ± 0.2	
0550671001	2009 Mar 16	27.3/20.0	54906.25	11.55883 (39)	71 ± 10	3.26 ± 0.28	0.73 ± 0.06	0.37 ± 0.06	0.63 ± 0.07	0.8 ± 0.3	
0550671101	2009 Mar 25	18.9/0	54915.66	11.55876 (52)							
0550671201	2009 Mar 23	27.1/15.7	54913.58	11.55861 (35)	75 ± 10	3.68 ± 0.30	0.67 ± 0.06	0.44 ± 0.07	0.57 ± 0.06	0.8 ± 0.3	
0550671301	2009 Apr 04	26.2/20.1	54925.54	11.55886 (36)	76 ± 10	3.64 ± 0.30	0.63 ± 0.05	0.47 ± 0.08	0.54 ± 0.06	0.7 ± 0.2	
0550671801	2009 Apr 22	28.2/28.2	54943.89	11.55903 (39)	60 ± 11	3.84 ± 0.28	0.62 ± 0.05	0.47 ± 0.08	0.54 ± 0.04	0.7 ± 0.2	
0550671901	2009 Apr 10	30.7/14.4	54931.53	11.55868 (37)	77 ± 12	3.56 ± 0.37	0.64 ± 0.07	0.45 ± 0.10	0.56 ± 0.06	0.7 ± 0.3	

NOTE. —  $f_p$  is the pulsed fraction after background subtraction ( $1\sigma$  uncertainty).  $\Gamma$  is the photon index inferred from the *power-law* model ( $\chi^2_{\nu}$  (d.o.f) = 1.48 (911));  $kT_{\text{bb}}$  and  $R_{\text{bb}}$  are the temperature and radius obtained from the *bbodyrad* model ( $\chi^2_{\nu}$  (dof) = 1.06 (911)).  $kT_{\text{RCS}}$  is the temperature obtained from the *RCS* model ( $\chi^2_{\nu}$  (dof) = 1.04 (909)) for strongly magnetized sources.  $F_X$  is the unabsorbed flux in 1–10 keV band in the *RCS* model. The errors of the last five columns are estimated at the 90% confidence level. The observation 0550671101 suffered from severe contamination of flares and is used only for determining  $P$  and  $\dot{P}$ .

<sup>a</sup> The exposure time of the flare-unscreened/flare-screened data.

<sup>b</sup> The start epoch of the flare-unscreened data after barycentric correction.

<sup>c</sup> The  $1\sigma$  uncertainty (Leahy 1987) of the last two digits is given in parentheses.

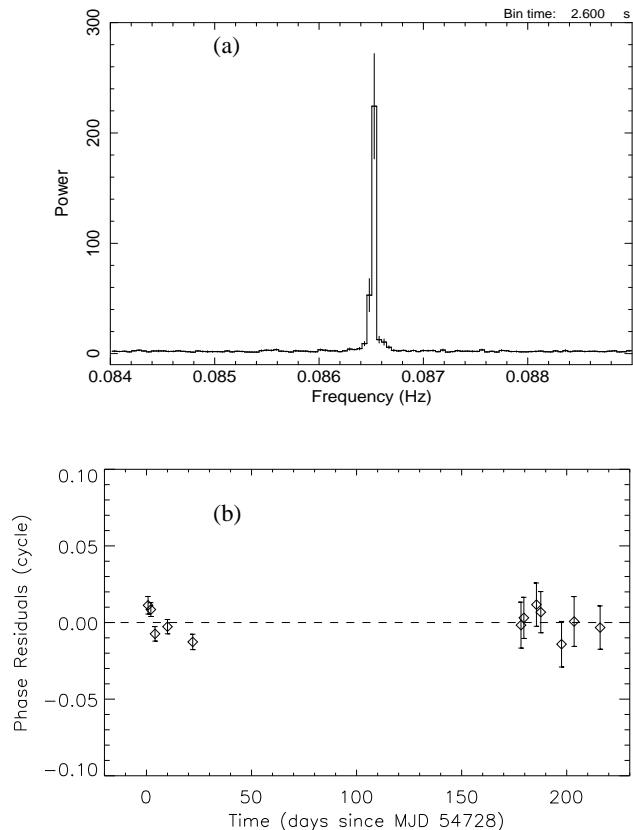


FIG. 2.— (a): the averaged power spectrum for the 12 time series of 3XMM J185246.6+003317 reveals a highly significant period at around 0.0865 Hz (11.56 s). (b): phase residuals for the 12 observations after subtraction of best-fit model ( $P = 11.5587126(4)$  s at MJD 54728.75 and  $\dot{P} = 5.7 \pm 4.8 \times 10^{-14}$  s s $^{-1}$ ).

the source was under the detection limit of *XMM-Newton* in 2004–2007 and up to the observation taken in 2007 March 20–21, it brightened during the 2008 September 19 observation (see Figure 1), and continued being detectable until 2009, according to the 16 archival *XMM-Newton* observations which covered the source. This indicates that this is a variable or transient source.

We reduced the *XMM-Newton* data using the Science Analysis System software (SAS)<sup>10</sup>. We then used XRONOS (version 5.22) and XSPEC (version 12.7.1) packages in HEASOFT<sup>11</sup> software (version 6.12) for timing and spectral analysis, respectively.

### 3. TIMING ANALYSIS

We first converted the photon arrival times to the solar system barycenter using the source coordinates R.A. = 18<sup>h</sup>52<sup>m</sup>46<sup>s</sup>.6, decl<sub>dot</sub> = 00°33′20″9, and then searched in the 12 observations for a periodicity in the power spectrum (*powspec*; 0.3–10 keV). As shown in Figure 2(a), we found a periodicity at  $P = 11.56$  s with high significance. To refine the estimated period, we used an epoch-folding method (*efsearch*) and searched periodicities around 11.56 s with a step of  $10^{-5}$  s. We determined the best-fit period<sup>12</sup> and uncertainty in each observation (listed in Table 1) by using a least squares fit of a Gaussian to the observed  $\chi^2$  value versus the period (Leahy 1987).

We subsequently constructed a phase-connected timing solution with the observations spanning seven months. To determine the time-of-arrival (TOA), we folded the time series using a fixed period  $P = 11.55871$  s for each piece of data in the 0.3–10 keV energy band. Using the single period is possible in this case since it

<sup>10</sup> <http://xmm.esac.esa.int/sas/>

<sup>11</sup> <http://heasarc.gsfc.nasa.gov/lheasoft/>

<sup>12</sup> A similar period is obtained using the  $Z^2_1$  test (Buccheri et al. 1983).

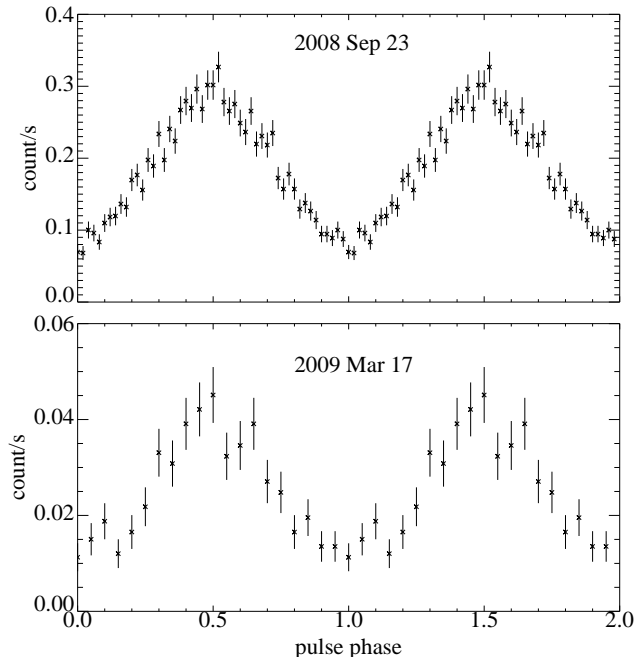


FIG. 3.— Folded light curves of 3XMM J185246.6+003317 in the 0.3–10 keV band from two *XMM-Newton* observations.

is consistent with the period measurements determined for all observations. A sinusoidal profile generally fitted the pulse profiles well and was thus used to estimate the TOAs. We first iteratively fitted the TOAs of the 12 observations to a linear ephemeris with the TEMPO2 software.<sup>13</sup> The model refines the period to  $P = 11.55871315(5)$  s, and gives an rms residual of  $\sim 0.9\%P$  ( $\chi^2/\text{degreesof freedom}(\text{dof}) = 25.4/10$ ). Adding a quadratic term gives a period  $P = 11.5587126(4)$  s for MJD 54728.75 and a spin-down rate  $\dot{P} = 5.7 \pm 4.8 \times 10^{-14} \text{ s s}^{-1}$  ( $1\sigma$  uncertainty), which slightly improves the fit ( $\chi^2/\text{dof} = 18.5/9$  and rms residual  $\sim 0.8\%P$ , see Figure 2(b)). Hereafter we use  $\dot{P} < 1.1 \times 10^{-13} \text{ s s}^{-1}$  due to the large error range of the best-fit  $\dot{P}$  value.

The period and the spin-down rate indicate a dipolar surface magnetic field  $B = 3.2 \times 10^{19} (P\dot{P})^{1/2} < 3.6 \times 10^{13}$  G. The characteristic age and the spin-down luminosity are  $\tau_c = P/(2\dot{P}) > 1.7$  Myr and  $\dot{E}_{\text{rot}} = 3.95 \times 10^{46} \dot{P} P^{-3} < 2.8 \times 10^{30} \text{ erg s}^{-1}$ , respectively.

We folded the light curves in the 0.3–10 keV band with 50 bins/period and 20 bins/period for the 2008 and 2009 observations (flare-screened), respectively (see Figure 3 for the pulse profiles). We also folded the light curves in the 0.3–2 keV and 2–10 keV bands to check for any variations, but we found no significant difference between the pulse profiles in the soft and hard bands. The pulsed fractions  $f_p$  after background subtraction are  $\sim 56\%$ – $77\%$  (see Table 1). Here  $f_p$  is defined as the count rate ratio of the pulsed emission to the total emission, and the lowest bin in the folded light curve was taken to represent the unpulsed level.

<sup>13</sup> <http://www.atnf.csiro.au/research/pulsar/tempo2/>

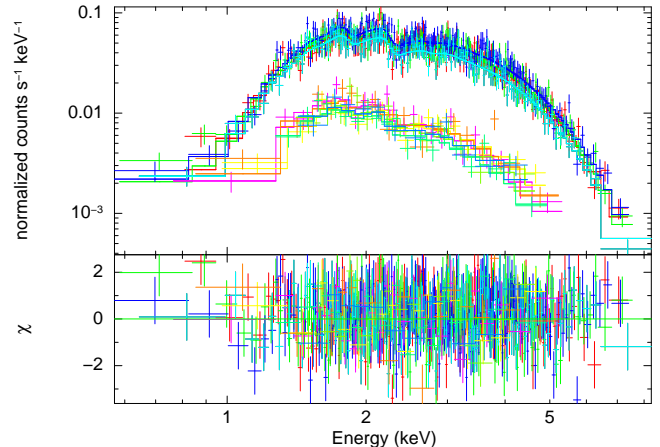


FIG. 4.— *XMM-Newton* EPIC-MOS2 spectra of the 11 observations (see Table 1) fitted by the RCS model, colored black, red, green, blue, light blue, magenta, yellow, orange, yellow+green, green+cyan, blue+cyan, and blue+magenta in the sequence of the observation ID. The upper and lower spectra are from the 2008 and 2009 observations, respectively. See Table 1 for a summary of the observations shown and the corresponding spectral parameters.

#### 4. SPECTRAL ANALYSIS

We extracted the 11 flare-screened EPIC-MOS2 spectra of 3XMM J185246.6+003317 from a circular region centered at the newly discovered source within a radius of  $30''$  with the local background subtracted from a nearby source-free region. All spectra were then adaptively binned to reach a background-subtracted signal-to-noise ratio of at least four.

We performed a joint-fit to the 11 spectra in the 0.3–10 keV energy range. For the foreground interstellar absorption, we applied the *phabs* model with the Anders & Grevesse (1989) abundances and the photo-electric cross-sections from Balucinska-Church & McCammon (1992). We first adopt absorbed *power-law* and *bbodyrad* (a blackbody model) models to fit the spectra, respectively, with a common absorption column density  $N_{\text{H}}$  for all spectra. The *power-law* model does not reproduce the spectra well ( $\chi^2_{\nu}$  (dof)=1.48 (911)) with the photon index ranging from 3.1 to 3.9. The single *bbodyrad* model with the foreground absorption  $N_{\text{H}} = 1.37 \pm 0.05 \times 10^{22} \text{ cm}^{-2}$  provides a good fit ( $\chi^2_{\nu}$  (dof)=1.06 (911)), noting that it under-estimates the hard X-ray tail above  $\sim 6$  keV. Adding a power-law or a blackbody component was not however statistically needed, given that only a few bins are above 6 keV and in the two-component model (*blackbody* + *blackbody* or *blackbody* + *power-law*) the parameters of the hard component were not well constrained.

We subsequently applied the resonant cyclotron scattering (RCS) model (Rea et al. 2008; Lyutikov & Gavril 2006), which accounts for RCS of the thermal surface emission by the hot magnetospheric plasma. This model has been successfully applied to a sample of magnetar spectra (Rea et al. 2008). The RCS model with  $N_{\text{H}} = 1.51 \pm 0.07 \times 10^{22} \text{ cm}^{-2}$  (constrained to be the same in all the observations) provided the best fit to the spectra ( $\chi^2_{\nu}$  (dof)=1.04 (909), the optical depth in the scattering slab  $\tau_{\text{res}} = 1\text{--}3$  and thermal velocity of the magnetospheric electrons  $\beta = 0.28^{+0.07}_{-0.15}c$ ), suggest-

ing a magnetar nature of the source. Figure 4 shows the spectra fitted with this model, and Table 1 summarizes the best fit results of the *power-law*, *bbodyrad* and RCS models, including the power-law photon index  $\Gamma$ , the blackbody temperature  $kT_{bb}$  and the corresponding radiating radius  $R_{bb}$  inferred from the *bbodyrad* model, the temperatures  $kT_{rcs}$  and the 1–10 keV unabsorbed X-ray fluxes  $F_X$  estimated from the best fit RCS model.

As shown in Table 1, the X-ray properties of 3XMM J185246.6+003317 varied over the seven month timescale covered by the 11 observations. The flux decreased by a factor of  $\sim 6$ , along with a decrease of the temperature from  $\sim 0.8$  keV to  $\sim 0.6$  keV according to the *bbodyrad* model, and from  $\sim 0.7$  keV to  $\sim 0.5$  keV based on the RCS model. Using the blackbody model, we find that the size of the emitting area,  $R_{bb}$ , varied between  $\sim 0.7$  km and  $\sim 0.4$  km (at a distance of 7.1 kpc, see details in Section 5), a value much smaller than the typical radius of a neutron star ( $\sim 10$  km). This indicates that the blackbody X-ray emission is emitted from a small area (e.g., a hot spot) rather than from the whole surface of the neutron star.

## 5. DISCUSSION

We discovered a new transient 11.56-s X-ray pulsar coincident with the point source 3XMM J185246.6+003317 in the *XMM-Newton* Serendipitous Source Catalogue and located south of SNR Kes 79. In this section, we further point out its low-B magnetar nature.

The previous *XMM-Newton* observations in 2004 and 2007 did not detect 3XMM J185246.6+003317. Neither was it detected in an archival *Chandra* observation taken in 2001 (ObsID 1982), nor in the *Chandra* source catalog (release 1.1).<sup>14</sup> Also, it was not detected by *ROSAT* observations taken in 1996–1997, and does not appear in the WGA Catalog of *ROSAT* point sources.<sup>15</sup> We also checked all the archival *Swift* observations of 3XMM J185246.9+003318 taken from 2012 September 25 to 2013 September 27, and we do not detect the source with either the X-Ray Telescope or the Burst Alert Telescope. Furthermore, we have not found any optical or infrared counterpart within  $2'4$  (the  $1\sigma$  positional uncertainties for 90% of the points sources in the 3XMM catalog) radius of the source in the Digital Sky Survey-2, the AllWISE Source Catalog, the Two Micron All Sky Survey images and All-Sky Point Source Catalog, and the GLIMPSE I Spring '07 Catalog and Archive.

The foreground absorption given by the best-fit RCS model,  $N_H \simeq 1.5 \times 10^{22} \text{ cm}^{-2}$ , is consistent with that of SNR Kes 79 ( $1.54\text{--}1.78 \times 10^{22} \text{ cm}^{-2}$ , Sun et al. 2004;  $1.50\text{--}1.53 \times 10^{22} \text{ cm}^{-2}$ , Giacani et al. 2009), suggesting that 3XMM J185246.6+003317 is likely located at a distance similar to that of Kes 79. Hence, we adopt a distance  $d$  of 7.1 kpc toward 3XMM J185246.6+003317, the same as that inferred for Kes 79 (Case & Bhattacharya 1998; Frail & Clifton 1989), and subsequently parameterize the physical properties with  $d/7.1$  kpc.

The data show a spectral evolution of the new source. The average X-ray flux of 3XMM J185246.6+003317 in the 1–10 keV band was around  $4.6 \times 10^{-12} \text{ erg s}^{-1}$  in 2008 and decreased to around  $7.8 \times 10^{-13} \text{ erg s}^{-1}$  in

2009. The corresponding luminosities are thus inferred to be  $L_X \approx 2.8 \times 10^{34} (d/7.1 \text{ kpc})^2 \text{ erg s}^{-1}$  and  $4.7 \times 10^{33} (d/7.1 \text{ kpc})^2 \text{ erg s}^{-1}$ , respectively, both of which rule out rotational energy loss ( $< 2.8 \times 10^{30} \text{ erg s}^{-1}$ ) as the source of the X-ray emission. This is one of the defining properties of magnetars. Along with the variation of the luminosity, the temperature  $kT_{bb}$  and the X-ray emitting radius  $R_{bb}$  in the blackbody scenario decreased as the flux decreased. The softening of the X-ray emission has been observed in transient magnetars during the outbursts decay (see, e.g., Rea & Esposito 2011).

We have thus provided firm evidence for 3XMM J185246.6+003317 being a new, transient magnetar, namely the slow pulsations, the X-ray luminosity higher than the spin-down power, the X-ray spectra characterized by a blackbody/RCS model that softened as the luminosity decreased, the lack of detection of any optical or infrared counterpart, and non-detection in archival X-ray observations prior to the 2008 September 19 *XMM-Newton* observation.

With a period of 11.5587126 (4) s (at MJD 54728.75), 3XMM J185246.6+003317 has the second longest period among currently known magnetars (after AXP 1E 1841–045 with  $P = 11.78$  s; Vasisht & Gotthelf 1997) and the longest period among the nine known transient magnetars. The low dipolar magnetic field  $B < 3.6 \times 10^{13}$  G deduced from the period and period derivative suggests that this is the third low-B magnetar discovered so far, joining SGR 0418+5729 and Swift J1822.3–1606.

Given that the source was not detected during the 2007 March 20 *XMM-Newton* observation but clearly detected in the 2008 September 19 observation, we conclude that an outburst likely occurred between these two periods. It is unclear when the outburst of 3XMM J185246.6+003317 started prior to the 2008 observation and whether the source was entering the quiescent stage during 2009. Since the spectrum of 3XMM J185246.6+003317 during the 2008–2009 observations did not require an additional power-law or hotter blackbody component, as is commonly observed (although with a few exceptions) in magnetars in quiescence, including 1E 1841–045 (Kumar & Safi-Harb 2010; Olausen & Kaspi 2013) and since the source is currently not detected by *SWIFT*, the source should remain in the outburst decay phase during the *XMM-Newton* observations reported here. Indeed, the blackbody component dominates the emission for a handful of magnetars during the later phases of the outburst decay (Rea & Esposito 2011). Moreover, the non-detection of 3XMM J185246.6+003317 in the X-ray observations before 2007 March 20 supports that the source was in quiescent state. The non-detection of it by *Chandra* ACIS-I during 2001 sets the  $3\sigma$  upper limit of the source's count rate to  $1 \times 10^{-3} \text{ counts s}^{-1}$  (1–10 keV), which corresponds to an unabsorbed flux  $6 \times 10^{-14} \text{ erg cm}^{-2} \text{ s}^{-1}$  (assuming  $N_H = 1.5 \times 10^{22} \text{ cm}^{-2}$  and a temperature  $kT_{bb} = 0.1$  keV that is similar to that inferred for the low-B magnetar Swift J1822.3–1606 during quiescence; Scholz et al. 2012; a lower flux would be obtained if the quiescent temperature is larger). The luminosity of 3XMM J185246.6+003317 in its quiescent stage is thus roughly estimated to be  $< 4 \times 10^{32} \text{ erg s}^{-1}$  (1–

<sup>14</sup> <http://cxc.harvard.edu/csc/>

<sup>15</sup> <http://heasarc.gsfc.nasa.gov/wgacat/>

10 keV), which is a factor of over 70 lower than that during 2008. This significant flux variation was commonly seen in several other magnetar outbursts. One explanation of the outburst involves the fast release of the energy in the crust (Lyubarsky et al. 2002). Another explanation is given by the untwisting magnetosphere model, which predicts a hot spot forms at the foot-prints of the current-carrying bundle of field lines, and the spot shrinks with the decrease of luminosity and temperature (Beloborodov 2009). It can interpret the decreased emitting area ( $R_{\text{bb}}$  from  $\sim 0.7$  km to  $\sim 0.4$  km) along with the spectral evolution found in this study.

It is well known that a 105 ms X-ray pulsar CXOU 185238.6+004020 (Seward et al. 2003) is located at the center of SNR Kes 79, and is identified as an “anti-magnetar” with a dipole magnetic field  $B = 3.1 \times 10^{10}$  G (Gotthelf et al. 2005; Halpern et al. 2007; Halpern & Gotthelf 2010). Considering the similar  $N_{\text{H}}$  inferred for both 3XMM J185246.6+003317 and Kes 79, it would be interesting to explore whether CXOU 185238.6+004020 or 3XMM J185246.6+003317 is associated with Kes 79. Note that in both cases the two objects could once be in a binary system or have no relation with each other. Given a dynamical age  $t_{\text{SNR}} \sim 5.4\text{--}7.5$  kyr (Sun et al. 2004) or a Sedov age  $\sim 5$  kyr (P. Zhou et al., in preparation) for SNR Kes 79, if 3XMM J185246.6+003317 was formed from the supernova that produced Kes 79, its projected velocity would be  $\sim 3 \times 10^3 (t_{\text{SNR}}/5 \text{ kyr})^{-1} \text{ km s}^{-1}$ . This velocity is very high when compared to the mean measured velocity of a sample of six magnetars ( $200 \pm 90 \text{ km s}^{-1}$ ; Tendulkar et al. 2013). Nevertheless, a high velocity has been proposed for another magnetar ( $1100 \text{ km s}^{-1}$  for SGR 0526–66 if associated with SNR N49; Park et al. 2012), and there is accumulating evidence for high pulsar speed, even exceeding  $4 \times 10^3 \text{ km s}^{-1}$  (e.g., Zou et al.

2005). However, the magnetar has a characteristic age  $\tau_c > 1.7$  Myr, and the low quiescent luminosity ( $< 4 \times 10^{32} \text{ erg s}^{-1}$ , assuming  $kT_{\text{bb}}=0.1$  keV) suggests a large age of the magnetar (0.1–1 Myr) estimated from a magneto-thermal evolution model (Viganò et al. 2013), which makes the association rather unlikely. Future monitoring observations and a proper motion measurement of 3XMM J185246.6+003317 are needed to confirm or refute this interesting scenario.

*Note added in manuscript.*—Fifteen days after our Letter was posted on arXiv on 2013 October 29 and while it was under revision, Rea et al. (2013) posted a Letter on this source. They independently confirmed our findings and the low-B magnetar nature of this source.

We gratefully acknowledge the anonymous referee for suggestions regarding phase-connected timing analysis and for comments that helped improve the Letter. We thank Tomaso Belloni, Michael Nowark, Wen-Fei Yu, Fang-Jun Lu, and Zhong-Xiang Wang for helpful discussions. We also thank Nanda Rea, Shuang-Nan Zhang, Ren-Xin Xu, Jin-Lin Han, Na Wang, Thomas Tauris, and Shriharsh P. Tendulkar for valuable comments, Song Huang for checking any optical/infrared counterpart, and Harsha Kumar for checking the *Swift* observations. P.Z. is grateful to the COSPAR Capacity Building Workshop, 2013. Y.C. and X.D.L. are grateful for the support from the 973 Program grant 2009CB824800, NSFC grants 11233001, 11133001, and 11333004, the grant 20120091110048 by the Educational Ministry of China, and the Qinglan Project of Jiangsu Province. S.S.H. acknowledges support from NSERC through the Canada Research Chairs Program and a Discovery Grant, and from the Canadian Space Agency, the Canadian Institute for Theoretical Astrophysics, and Canada’s Foundation for Innovation.

## REFERENCES

- Alpar, M. A. Çalıřkan, Ş. & Ertan, Ü. 2013, in IAU Symp. 290, Neutron Stars, fallback Disks, Magnetars, eds. C. M. Zhang, T. Belloni, M. Méndez, S. N. & Zhang (Cambridge: Cambridge Univ. Press), 93
- Anders, E., & Grevesse, N. 1989, *GeCoA*, 53, 197
- Balucinska-Church, M., & McCammon, D. 1992, *ApJ*, 400, 699
- Beloborodov, A. M. 2009, *ApJ*, 703, 1044
- Buccheri, R., Bennett, K., Bignami, G. F., et al. 1983, *A&A*, 128, 245
- Camilo, F., Ransom, S. M., Halpern, J. P., et al. 2006, *Natur*, 442, 892
- Case, G. L., & Bhattacharya, D. 1998, *ApJ*, 504, 761
- Chen, Y., Jiang, B., Zhou, P., et al. 2013, arXiv:1304.5367
- Frail, D. A., & Clifton, T. R. 1989, *ApJ*, 336, 854
- Gavriil, F., Gonzalez, M. E., Gotthelf, E. V., et al. 2008, *Sci*, 319, 1802
- Giacani, E., Smith, M. J. S., Dubner, G., et al. 2009, *A&A*, 507, 841
- Gotthelf, E. V., Halpern, J. P. & Seward, F. D. 2005, *ApJ*, 627, 390
- Gotthelf, E. V., Halpern, J. P. & Alford, J. 2013, *ApJ*, 765, 58
- Halpern, J. P., Gotthelf, E. V., Camilo, F. & Seward, F. D. 2007, *ApJ*, 665, 1304
- Halpern, J. P., & Gotthelf, E. V. 2010, *ApJ*, 709, 436
- Ibrahim, A. I., Markwardt, C. B., Swank, J. H., et al. 2004, *ApJL*, 609, L21
- Kumar, H. S. & Safi-Harb, S. 2008, *ApJL*, 678, L43
- Kumar, H. S. & Safi-Harb, S. 2010, *ApJL*, 725, L191
- Leahy, D. A. 1987, *A&A*, 180, 275
- Lyubarsky, Y., Eichler, D., & Thompson, C. 2002, *ApJL*, 580, L69
- Lyutikov, M., & Gavriil, F. P. 2006, *MNRAS*, 368, 690
- Mereghetti, S. 2008, *A&A Rev.*, 15, 225
- Mereghetti, S. 2013, *BrJPh*, 38
- Olausen, S. A., & Kaspi, V. M. 2013, arXiv:1309.4167
- Ouyed, R., Leahy, D. & Niebergal, B. 2007, *A&A*, 473, 357
- Park, S., Hughes, J. P., Slane, P. O., et al. 2012, *ApJ*, 748, 117
- Rea, N. 2013, in IAU Symp. 291, Neutron Stars and Pulsars: Challenges and Opportunities after 80 Years, ed. J. van Leeuwen (Cambridge: Cambridge Univ. Press), 11
- Rea, N. & Esposito, P. 2011, in *Astrophysics and Space Science Proceedings, High-Energy Emission from Pulsars and their Systems*, ed. D. F. Torres, & N. Rea, (Berlin: Springer), 247
- Rea, N., Esposito, P., Turolla, R., et al. 2010, *Science*, 330, 944
- Rea, N., Israel, G. L., Esposito, P., et al. 2012, *ApJ*, 754, 27
- Rea, N., Viganò, D., Israel, G. L., Pons, J. A., & Torres, D. F. 2013, arXiv:1311.3091
- Rea, N., Zane, S., Turolla, R., Lyutikov, M., & Götz, D. 2008, *ApJ*, 686, 1245
- Scholz, P., Ng, C.-Y., Livingstone, M. A., et al. 2012, *ApJ*, 761, 66
- Seward, F. D., Slane, P. O., Smith, R. K., & Sun, M. 2003, *ApJ*, 584, 414
- Struder, L., Briel, U., Dennerl, K., et al. 2001, *A&A*, 365, L18
- Sun, M., Seward, F. D., Smith, R. K., & Slane, P. O. 2004, *ApJ*, 605, 742
- Tendulkar, S. P., Cameron, P. B., & Kulkarni, S. R. 2013, *ApJ*, 772, 31
- Thompson, C., & Duncan, R. C. 1995, *MNRAS*, 275, 255
- Thompson, C., & Duncan, R. C. 1996, *ApJ*, 473, 322

Thompson, C., Lyutikov, M., & Kulkarni, S. R. 2002, *ApJ*, 574, 332  
Turner, M. J. L., Abbey, A., Arnaud, M., et al. 2001, *A&A*, 365, L27  
Vasisht, G., & Gotthelf, E. V. 1997, *ApJL*, 486, L129

Viganò, D., Rea, N., Pons, J. A., et al. 2013, *MNRAS*, 434, 123  
Zou, W. Z., Hobbs, G., Wang, N., et al. 2005, *MNRAS*, 362, 1189